Journal of The Electrochemical Society, **155** (8) H563-H568 (2008)
0013-4651/2008/155(8)/H563/6/$23.00 © The Electrochemical Society

Formation of High-Quality Ag-Based Ohmic Contacts to p-Type GaN

Ho Won Jang, Jun Ho Son, and Jong-Lam Lee[z]

Department of Materials Science and Engineering, Pohang University of Science and Technology (POSTECH), Pohang, Gyungbuk 790-784, Korea

Low resistance and high reflectance ohmic contacts on p-type GaN were achieved using an Ag-based metallization scheme. Oxidation annealing was the key to achieve ohmic behavior of Ag-based contacts on p-type GaN. A low contact resistivity of $\sim 5 \times 10^{-5}$ Ω cm^2 could be achieved from Me (=Ni, Ir, Pt, or Ru)/Ag (50/1200 Å) contacts after annealing at 500°C for 1 min in O_2 ambient. Oxidation annealing promoted the out-diffusion of Ga atoms from the GaN layer, and Ga atoms dissolved in the in-diffused Ag layer with the formation of Ag–Ga solid solution, resulting in ohmic contact formation. Using Ru/Ni/Au (500/200/500 Å) overlayers on the Me/Ag contacts, the excessive incorporation of oxygen molecules into the contact interfacial region, and the out-diffusion and agglomeration of Ag, were effectively prevented during oxidation annealing. As a result, a high reflectance of 87.2% at the 460 nm wavelength and a smooth surface morphology could be obtained simultaneously.
 [DOI: 10.1149/1.2940324]

Manuscript submitted April 25, 2008; revised manuscript received May 16, 2008. Available electronically June 18, 2008.

There has been great interest in metal contacts to GaN and related alloys for application to light-emitting diodes (LEDs) operating in the visible and UV regions. Metal contacts play an important role in device performance, such as light extraction efficiency, power consumption, and reliability.[1] Achieving low resistance ohmic contacts to n-type GaN is relatively easy using Ti/Al-based metallization schemes,[2-4] but ohmic contacts to p-type GaN are much more difficult to achieve due to the low activation efficiency of Mg dopants in GaN.[5] A wide variety of metallization schemes with high work function metals such as Ni,[6-9] Pd,[10-12] Pt,[13-15] Ru,[16,17] Ir,[18] and Rh[19] has been employed to achieve low resistance ohmic contacts to p-type GaN. Among those schemes, Ni/Au is commonly used as a p-type ohmic electrode for GaN-based LEDs due to its reliably low contact resistivity and high light transmittance.[20-22]

Recently, vertical-structure designs fabricated by laser lift-off have been reported to be very effective for increasing the light extraction efficiency of GaN-based LEDs.[23,24] In these configurations, achieving high reflectance and low resistance ohmic contacts to p-type GaN is essential for improving device performance. Conventional Au-based ohmic contacts such as Ni/Au, Pd/Au, and Pt/Au are not appropriate for those devices because the light reflectance of Au is below 40% in the blue wavelength region.[25] Ag has the highest reflectivity in the visible wavelength region. However, it is difficult to achieve high-quality Ag-based ohmic contacts to p-type GaN. For example, even though direct Ag contact to p-type GaN can produce ohmic behavior with a specific contact resistivity of $\sim 10^{-4}$ Ω cm^{-2}, it suffers from poor mechanical adhesion and thermal instability such as agglomeration, void formation, and oxidation during postannealing.[26] While various contact schemes using interlayers and/or overlayers have been reported to solve these problems,[27-33] achieving high-quality Ag-based ohmic contacts to p-type GaN is still challenging.

In this work, we report Ag-based ohmic contacts to p-type GaN that have low resistance and high reflectance. To find the effect of oxidation annealing on the reduction of contact resistivity, the contacts were annealed separately in O_2 and N_2 ambient. Interfacial reactions between contact metals and GaN were analyzed through depth profiles of secondary ion mass spectroscopy (SIMS). Synchrotron photoemission spectroscopy (SRPES) was employed to determine chemical shifts in the contact metals after annealing. We propose a mechanism for the ohmic contact formation of Ag-based contacts to p-type GaN based on these experimental results. Finally, we present an Ag-based metallization scheme with highly improved reflectance and smooth surface morphology.

[z] E-mail: jllee@postech.ac.kr

Experimental

Mg-doped p-type GaN films used in this work were grown on (0001) sapphire substrate using metallorganic chemical vapor deposition (MOCVD). The net hole concentration was determined to be 3×10^{17} cm^{-3} by Hall measurements. For the measurement of specific contact resistivity using the transmission line method (TLM), active regions were defined by inductively coupled plasma etching using Cl_2/BCl_3 gas, followed by dipping the samples into a boiling aqua regia solution of $HCl:HNO_3$ (3:1) to remove surface native oxides formed during MOCVD and/or rapid thermal annealing.[10] A TLM test structure with 100×50 μm pads was patterned on the surface-treated samples using a photoresist. Prior to metal deposition, all the samples were dipped in HCl:DI (1:1) solution for 2 min. After the HCl treatment, contact metals were deposited on p-type GaN by electron beam evaporation under a base pressure of 2×10^{-7} Torr. After lift-off of metals deposited on the photoresist, the samples were annealed at temperatures ranging from 300 to 800°C for 1 min in N_2 and O_2 ambient. Current–voltage (I-V) characteristics of the contacts were examined using a semiconductor parameter analyzer. Light reflectance of the contacts was measured using a monochromator equipped with a xenon lamp. In measurements of reflectance, a reflected beam at an incidence angle of 45° was collimated to a photomultiplier tube. An Ag mirror with a certified reflectance of over 96% in the wavelength range was used as a reflectance standard.

SRPES measurements were carried out in the 8A1 beamline at Pohang Accelerator Laboratory. The energy resolution of binding energy in the SRPES measurements was ±0.05 eV. The binding energy was calibrated using Au Fermi levels and peak positions of Au 4f core levels obtained from a Au foil. Plane-view scanning electron microscopy (SEM) and cross-section transmission electron microscopy (TEM) images were obtained to examine surface morphology and interface structure, respectively.

Results

Bilayer ohmic contacts.— Figure 1 shows contact resistivities of Ni (50 Å)/Ag (1200 Å) contacts as a function of annealing temperature in N_2 and O_2 ambient. N_2-annealed samples showed a nonlinear rectifying behavior, but O_2-annealed samples showed linear ohmic characteristics after annealing at 400–600°C. Compared with N_2-annealed samples, the reduction of contact resistivity by three orders of magnitude was achieved from O_2-annealed samples. This result indicates that apparently oxidation annealing is of vital importance to achieve ohmic behavior of Ni/Ag contacts on p-type GaN. Figure 1b shows contact resistivities of Ni/Ag contacts with various Ni thicknesses as a function of annealing temperature. Except for Ni (20 Å)/Ag (1200 Å) contact, all contacts show their minimum contact resistivities after annealing at 500°C. The value of minimum

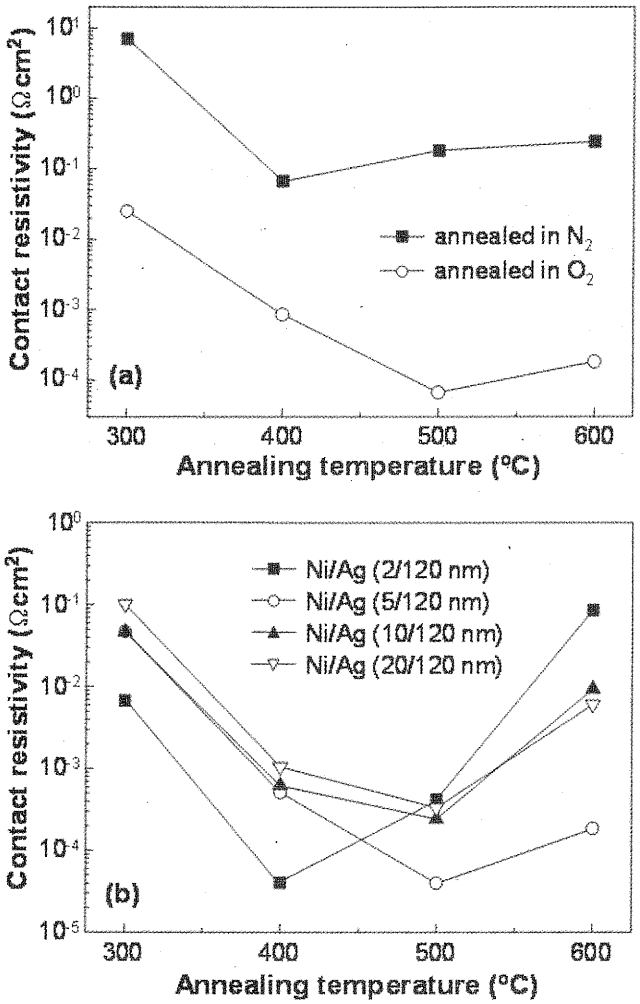

Figure 1. (a) Contact resistivities of Ni/Ag (50/1200 Å) contacts as a function of annealing temperature in N_2 and O_2 ambient. (b) Contact resistivities of the Ni/Ag contacts with different Ni thickness as a function of annealing temperature in O_2 ambient.

contact resistivity increased with Ni thickness. This result suggests that the optimization of the Ni thickness is very important for improving contact resistivities of Ni/Ag contacts on p-type GaN.

Instead of Ni, other metals such as Ir, Pt, and Ru were employed as a contact metal layer to investigate the effects of contact metal layers on the ohmic contact formation of the Ag-based contact scheme. Because the contact metals (Ni, Ir, Pt, and Ru) have high work functions (>5.0 eV) and much better adhesion to GaN compared with Ag, both contact resistivity and adhesion to GaN could be improved. Figure 2 displays *I-V* curves of Ni/Ag, Ir/Ag, Pt/Ag, and Ru/Ag (50/1200 Å) contacts after annealing at 500°C for 1 min in O_2 ambient. All contacts exhibited linear ohmic behaviors. Low contact resistivities of $\sim 5 \times 10^{-5}$ Ω cm^2 were achieved from all contacts independent of contact metal variation. This suggests that the contact metal layer is not a key aspect of the ohmic contact formation in the Ag-based contacts.

To study interfacial reactions during annealing, SIMS depth profiles of Ni/Ag contacts before and after annealing were obtained, shown in Fig. 3. When the contact was annealed in N_2 ambient, Ag in-diffused toward GaN. But, intermixing between metals and GaN was not considerable. After annealing in O_2 ambient, the intermixing was significant. Ag completely in-diffused and directly contacted with GaN. Thus, there was no abrupt interface between Ag and Ni. The oxygen profile coincided with the Ni profile, indicating the transformation of Ni into NiO. Compared with N atoms, the out-

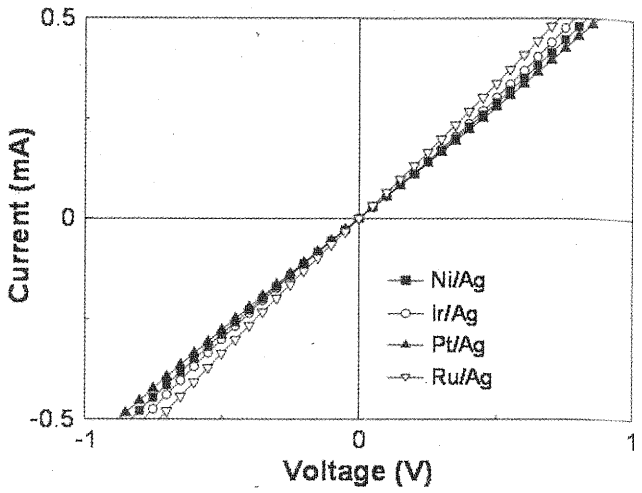

Figure 2. *I-V* curves of Ni/Ag, Ir/Ag, Pt/Ag, and Ru/Ag (50/1200 Å) contacts after annealing at 500°C in O_2 ambient.

diffusion of Ga atoms was more pronounced. The long diffusion tail of Ga in the Ag layer is a clear indicator of the dissolution of Ga atoms in Ag.

Figure 4 shows SRPES spectra of the Ag $3d_{5/2}$ core level for thin Ni (10 Å)/Ag (10 Å) contacts before and after annealing at 500°C. The peak intensity decreased gradually after annealing in N_2 and O_2 ambient, which resulted from Ag in-diffusion and/or agglomeration. The binding energy shifted toward lower energies after annealing. For the O_2-annealed sample, the energy shift was as high as 0.65 eV, which indicates the reduction of Schottky barrier height (SBH) for the transport of holes across the interface. Deconvolution of the Ag 3d spectra was performed to identify the bonding states of

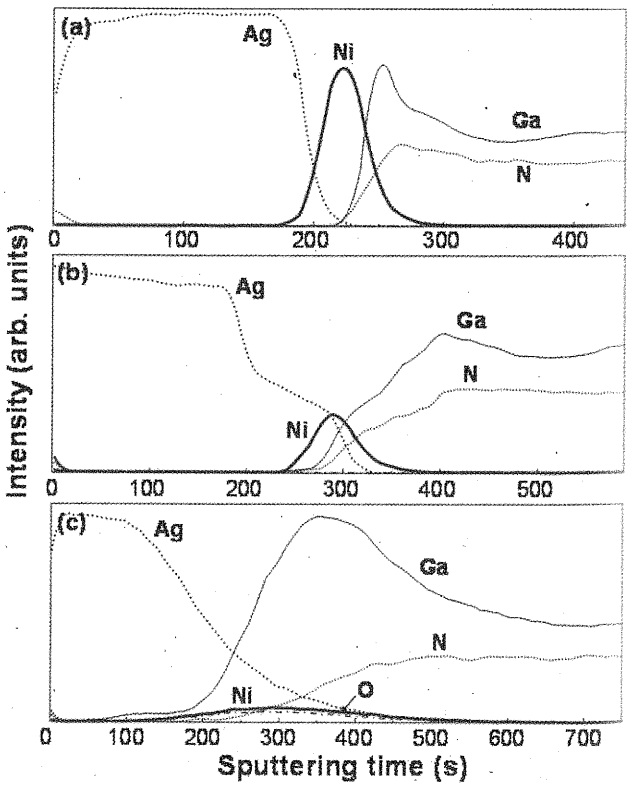

Figure 3. SIMS depth profiles of Ni/Ag (50/1200 Å) contacts: (a) as-deposited and annealed at 500°C in (b) N_2 and (c) O_2 ambient.

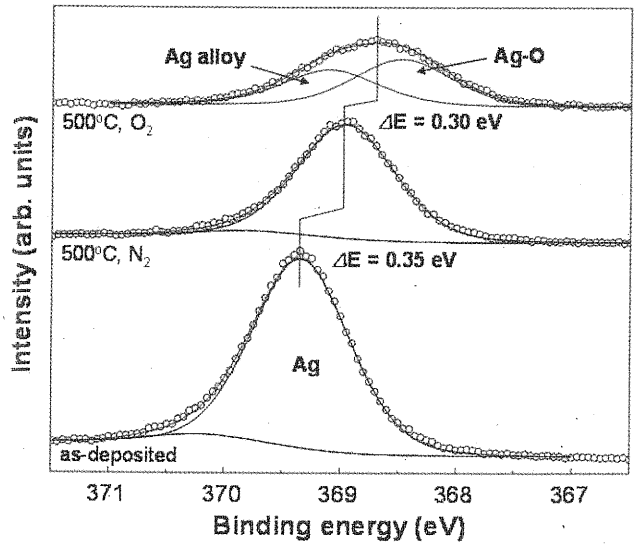

Figure 4. SRPES spectra of Ag $3d_{5/2}$ core levels for Ni/Ag (10/10 Å) contacts before and after annealing. The fwhm values of Ag 3d peaks were calculated to be 0.90, 0.89, and 1.15 eV for the as-deposited, N_2-annealed, and O_2-annealed contacts, respectively.

Ag on the p-type GaN layer. A Shirley background subtraction was applied to the spectra and mixed Gaussian–Lorentzian peaks were used in this analysis. The energy resolution of the deconvoluted peak position was ±0.1 eV. In the as-deposited condition, the Ag 3d spectrum was symmetric and nearly coincided with the fit line, indicating that the peak was mainly composed of a Ag–Ag metallic bond. The full width at half-maximum (fwhm) value of the fit line did not change for the N_2-annealed sample. This suggests that there was only a Ag–Ag bond after annealing in N_2 ambient. However, the fwhm value increased to 1.15 eV for the O_2-annealed sample. This means that additional bonding is superimposed in the Ag 3d spectrum. When the peak was deconvoluted into two bond states, corresponding to Ag–O and Ag alloy (Ag–Ga) bonds, the file line coincided with the original spectrum. Binding energy differences, 0.43 for $E_{Ag-Ga} - E_{Ag-Ag}$ and 0.20 eV for $E_{AgAg} - E_{Ag-O}$, are in good agreement with previously reported values.[34] The formation of Ag–O and Ag–Ga bonds indicates the oxidation of Ag and the formation of Ag–Ga solid solution, respectively. The formation of Ag–Ga solid solution after oxidation annealing is consistent with the SIMS result of the Ni (50 Å)/Ag (1200 Å) contact.

To examine the change of electronic properties of contact metals after annealing, spectra of secondary electron emission and valence band were obtained. Figure 5a shows onsets of secondary electron

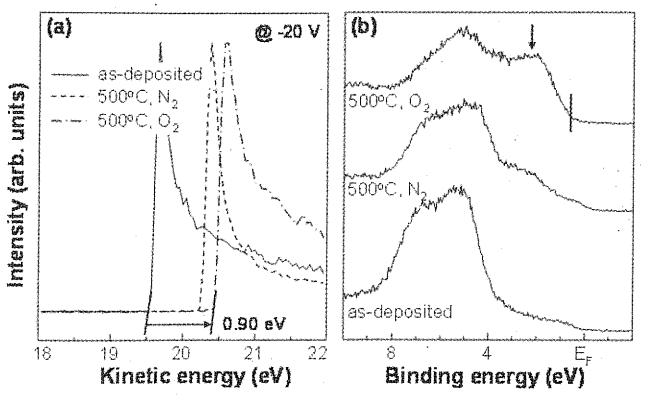

Figure 5. (a) Secondary electron emission and (b) valence band spectra for Ni/Ag (10/10 Å) contacts before and after annealing.

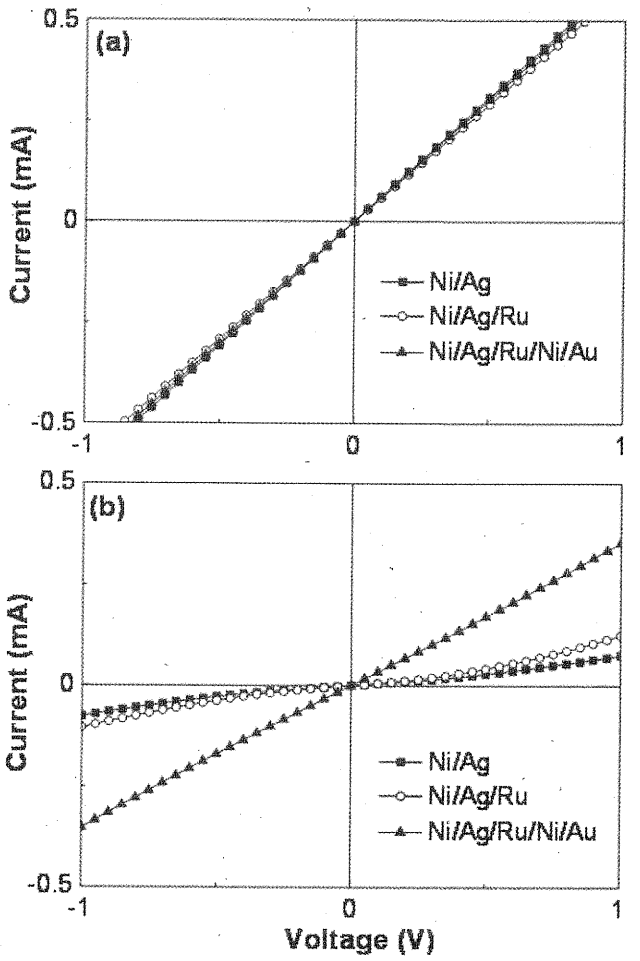

Figure 6. *I-V* curves of Ni/Ag (50/1200 Å), Ni/Ag/Ru (50/1200/500 Å), and Ni/Ag/Ru/Ni/Au (50/1200/500/200/500 Å) contacts after annealing at (a) 500°C and (b) 800°C in O_2 ambient.

emission of thin Ni (10 Å)/Ag (10 Å) contacts before and after annealing at 500°C. The onsets shifted toward higher kinetic energies after annealing. However, the shift was more pronounced in the O_2-annealed samples. This suggests that the increase of metal work function should be enhanced with the formation of metal oxides, in good agreement with previous reports.[17,18] Figure 5b shows valence band spectra of thin Ni (10 Å)/Ag (10 Å) contacts before and after annealing at 500°C. In the as-deposited sample, the valence band-edge does not coincide with the Fermi level because the metal thickness is not high enough to screen the photoemission-induced surface band bending of underlying p-type GaN.[35,36] After annealing in N_2 ambient, there was no considerable change in the position of the edge and spectrum shape, meaning that metallic properties of contact layers were preserved after annealing. When the samples were annealed in O_2 ambient, the edge shifted toward higher binding energies together with a change in the spectrum shape. This is indicative of the formation of metal oxides, namely, NiO and Ag_2O after oxidation annealing. It was found that the peak position of the hump at the binding energy of ~2.2 eV in the O_2-annealed Ni/Ag contact is very close to that of the Ni 3d valence.[34] This indicates that the surface of the oxidized Ni/Ag contact was primarily composed of NiO. Therefore, it is suggested that the oxidation annealing could cause a layer inversion reaction in the thin Ni/Ag contact, resulting in the contact structure of NiO/Ag/p-GaN.

Multilayer ohmic contacts.— Figure 6a displays *I-V* curves of Ni (50 Å)/Ag (1200 Å), Ni (50 Å)/Ag (1200 Å)/Ru (500 Å),

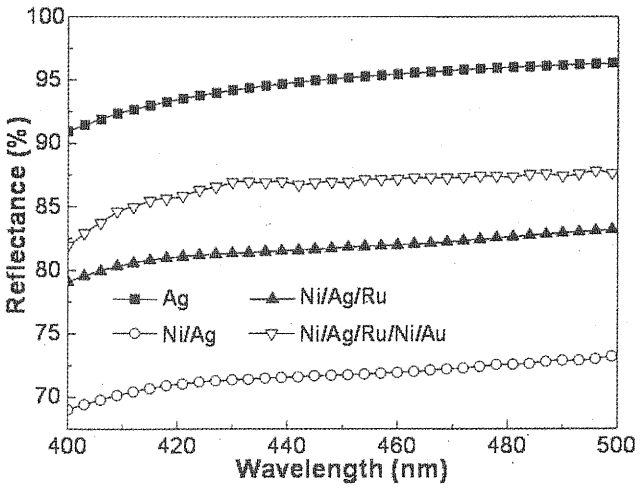

Figure 7. Light reflectance spectra of Ni/Ag (10/1200 Å), Ni/Ag/Ru (10/1200/500 Å), and Ni/Ag/Ru/Ni/Au (10/1200/500/200/500 Å) contacts after annealing at 500°C in O_2 ambient.

and Ni (50 Å)/Ag (1200 Å)/Ru (500 Å)/Ni (200 Å)/Au (500 Å) contacts after annealing at 500°C for 1 min in O_2 ambient. Three contacts exhibit almost identical *I-V* curves. Contact resistivity as low as $\sim 5 \times 10^{-5}$ Ω cm^2 could be obtained from all contacts. Figure 6b shows *I-V* curves of the three contacts after annealing at 800°C for 1 min in O_2 ambient. While the Ni/Ag and Ni/Ag/Ru contacts show a rectifying behavior, the Ni/Ag/Ru/Ni/Au contact still shows a linear ohmic behavior. This provides direct evidence of the superior thermal stability of the Ni/Ag/Ru/Ni/Au multilayer contact to the Ni/Ag and Ni/Ag/Ru contacts.

Figure 7 shows light reflectance spectra of the Ni/Ag, Ni/Ag/Ru, and Ni/Ag/Ru/Ni/Au contacts after annealing at 500°C in O_2 ambient. We reduced the thickness of Ni contact metal from 50 to 10 Å because Ni has a low reflectance (~54%) for visible light. For the Ni/Ag contact, the reflectance at the 460 nm wavelength was 71.9%. When the Ru overlayer was employed, the reflectance increased to 82.1% for the Ni/Ag/Ru contact. For the Ni/Ag/Ru/Ni/Au contact, the reflectance was measured to be 87.3%, one of the highest among previously reported values for reflective ohmic contacts on p-type GaN.[26-33] For the Ni/Ag contact, contact resistivities changed with various Ni thicknesses (shown in Fig. 1). No significant change in contact resistivity of the Ni/Ag/Ru/Ni/Au contact with the thickness of Ni contact layer was found (not shown here), because the Ru/Ni/Au overlayers effectively suppress excessive oxygen incorporation and Ag agglomeration during oxidation annealing.

SIMS depth profiles of the Ni/Ag/Ru and Ni/Ag/Ru/Ni/Au contacts after annealing at 500°C in O_2 ambient are shown in Fig. 8. For the Ni/Ag/Ru contact, the Ni contact layer was apparently transformed into NiO, similar to the Ni/Ag contact, and the Ru overlayer was also oxidized. The significant Ga out-diffusion and Ag in-diffusion are consistent with the SIMS result of the Ni/Ag contact. It was observed that Ag out-diffused to the surface through the Ru overlayer, which reveals that the Ru overlayer did not act as a diffusion barrier for both Ag out-diffusion and Ni oxidation by oxygen molecules from the ambient gas. For the Ni/Ag/Ru/Ni/Au contact, NiO was formed at the surface, resulting in the overlayer structure of Ru/Au/NiO. The in-diffusion of oxygen molecules stopped in the Ru layer, and thus there was no oxidation of the Ni contact layer. This means that the Ru/Ni/Au overlayer effectively suppressed excessive oxygen in-diffusion to the contact interface with GaN, preventing the oxidation of the Ni contact layer. Intermixing between Ag and GaN was also found, but no out-diffusion of Ag atoms to the surface was observed. This suggests that the Ru layer prevented Ag out-diffusion to the surface.

Figure 9 displays a cross-sectional TEM image of the Ni/Ag/Ru/

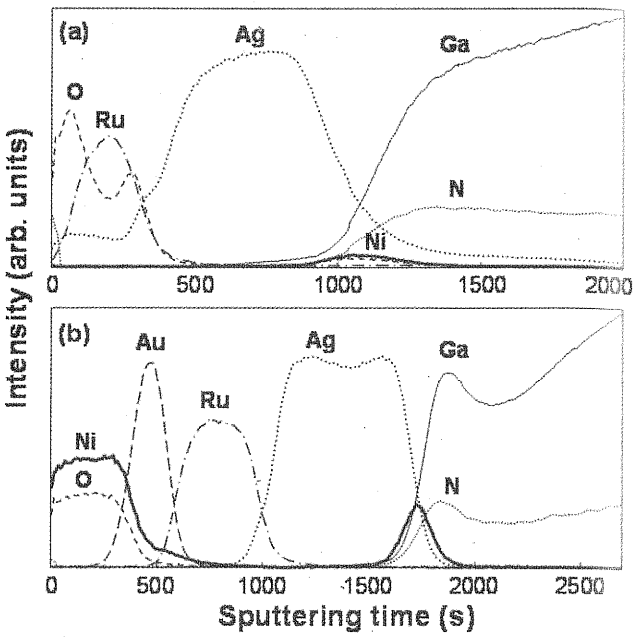

Figure 8. SIMS depth profiles of (a) Ni/Ag/Ru and (b) Ni/Ag/Ru/Ni/Au contacts after annealing at 500°C in O_2 ambient.

Ni/Au contact after annealing at 500°C in O_2 ambient. NiO was formed at the surface and covered the contact area completely, leading to the overlayer structure of Ru/Au/NiO which is consistent with the SIMS result in Fig. 8b. It is surprising that the interfaces of NiO/Au, Au/Ru, and Ru/Ag were abrupt after annealing. The layer-by-layer structure of NiO/Au/Ru/Ag/p-GaN clarifies the fact that the Ag layer acts as an effective reflector after oxidation annealing.

The surface morphology of reflective ohmic contacts must be smooth to guarantee good contact pattern definition and adhesion with metal overlayers. Figure 10 shows SEM images for surface morphologies of Ni/Ag, Ni/Ag/Ru, and Ni/Ag/Ru/Ni/Au contacts after oxidation annealing. For the Ni/Ag contact, the surface was very rough with irregular agglomerates. Agglomeration by annealing is a typical phenomenon in Ag films involving the evolution of capillary instabilities that leads to continuous uncovering of the substrate.[37] For the Ni/Ag/Ru contact, the surface was also rough with protrusions. The Ag out-diffusion through the oxidized Ru overlayer, as shown in Fig. 8a, resulted in the formation of the

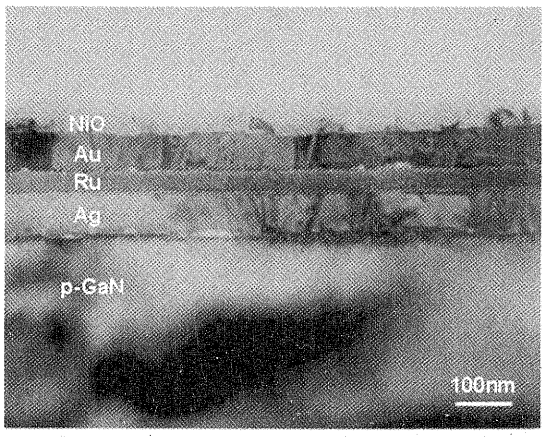

Figure 9. A cross-sectional TEM image of the Ni/Ag/Ru/Ni/Au contact after annealing at 500°C in O_2 ambient.

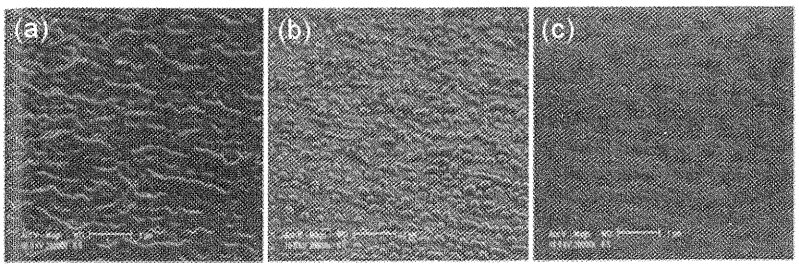

Figure 10. SEM images of surface morphology for the Ni/Ag, Ni/Ag/Ru, and Ni/Ag/Ru/Ni/Au contacts after annealing at 500°C in O_2 ambient (45° tilted).

protrusions at the surface. The surface of the Ni/Ag/Ru/Ni/Au contact was relatively smooth, which is attributed to the layer-by-layer contact structure in Fig. 9.

Discussion

First, the mechanism for the ohmic contact formation of Ni/Ag contacts on p-type GaN is discussed based on experimental results. The incorporated oxygen molecules during oxidation annealing accelerated the decomposition of GaN epilayers to form GaO_x due to the higher bonding strength of the Ga–O bond than that of the Ga–N bond, promoting Ga out-diffusion to metal layers.[21] After the oxidation annealing, Ag came into direct contact with the p-type GaN epilayer in Fig. 3. Then, Ga atoms from GaN dissolved in the Ag layer to form Ag–Ga solid solution due to the high solubility of Ga in Ag (~19% at 500°C).[38] Thus, the Ga out-diffusion was also promoted by Ag in-diffusion. Therefore, a number of Ga vacancies were created near the GaN contact interfacial region. Because Ga vacancies act as acceptors for electrons in GaN, the net hole concentration near the surface region increased and the surface Fermi level moved to the energy level of Ga vacancy. In addition, the metal work function increased after the oxidation annealing in Fig. 5. As a result, the depletion layer width below the contact and the effective SBH for the transport of holes decreased simultaneously, leading to the drastic reduction of contact resistivity in the oxidized Ni/Ag contacts on p-type GaN.

The significant improvement in both light reflectance and surface morphology for the Ni/Ag/Ru/Ni/Au multilayer ohmic contact is attributed to the Ru/Ni/Au overlayer. Oxygen molecules incorporated during oxidation annealing promoted the formation of Ag–Ga solid solution, resulting in ohmic contact formation. However, the excessive in-diffusion of oxygen molecules caused the severe Ag agglomeration, resulting in the rough surface morphology in Fig. 10a. The agglomeration of the Ag layer led to a decrease in light reflectance due to the light transmission through the thinner areas. When the Ni/Ag/Ru/Ni/Au contact was annealed in O_2 ambient, NiO was formed at the surface, accompanied with the layer inversion from Ni/Au to Au/NiO in Fig. 8b. Gibbs free-energy changes for the formation of NiO, RuO_2, and Ag_2O at 500°C are calculated to be −83.7, −57.2, and 7.0 kJ/mol, respectively.[39] This indicates that the formation of NiO is energetically favorable for the oxidized Ni/Ag/Ru/Ni/Au contact. Therefore, it is suggested that the excessive in-diffusion of oxygen molecules to the underlying Ru and Ag layers could be suppressed by the formation of NiO. Furthermore, the out-diffusion of Ag to the surface was prevented by the Ru layer. This led to the high reflectance and smooth surface morphology of the Ni/Ag/Ru/Ni/Au contact after oxidation annealing.

Conclusion

The formation of low resistance and high reflectance Ag-based ohmic contacts to p-type GaN was investigated. Independent of a variation of the contact metal, a low contact resistivity of $\sim 5 \times 10^{-5}$ Ω cm^2 was achieved from Me (=Ni, Ir, Pt, or Ru)/Ag (50/1200 Å) contacts after annealing at 500°C for 1 min in O_2 ambient. Oxidation annealing promoted the out-diffusion of Ga atoms from the GaN layer, and Ga atoms dissolved in the in-diffused Ag layer with the formation of Ag–Ga solid solution, resulting in the ohmic contact formation. Using Ru/Ni/Au (500/200/500 Å) overlayers on the Me/Ag contacts, a high reflectance of 87.2% at 460 nm wavelength and smooth surface morphology were obtained simultaneously. The overlayers suppressed the excessive incorporation of oxygen into the contact layers and the out-diffusion of Ag to the surface during oxidation annealing, leading to the high reflectance and smooth surface quality. It is suggested that the Me/Ag/Ru/Ni/Au contacts are very suitable for high-power GaN LEDs with vertical-structure configurations.

Acknowledgments

This work was supported in part by the Korean Research Foundation Grant funded by the Korean Government (MOEHRD) (KRF-2005-005-J13102), and in part by the second stage of the Brain Korea 21 Project in 2007.

Pohang University of Science and Technology assisted in meeting the publication costs of this article.

References

1. S. J. Pearton, J. C. Zolper, R. J. Shul, and F. Ren, *J. Appl. Phys.*, **86**, 1 (1999).
2. S. Fernández, R. Peña, M. T. Rodrigo, J. Plaza, M. Verdú, F. J. Sánchez, and M. T. Montojo, *Appl. Phys. Lett.*, **90**, 083504 (2007).
3. T. Jang, S. N. Lee, O. H. Nam, and Y. Park, *Appl. Phys. Lett.*, **88**, 193505 (2006).
4. F. Iucolano, F. Roccaforte, A. Alberti, C. Bongiorno, S. D. Franco, and V. Raineri, *J. Appl. Phys.*, **100**, 123706 (2006).
5. Y.-J. Lin, *Appl. Phys. Lett.*, **84**, 2760 (2004).
6. C. L. Tseng, M. J. Youh, G. P. Moore, M. A. Hopkins, R. Stevens, and W. N. Wang, *Appl. Phys. Lett.*, **83**, 3677 (2003).
7. J. O. Song, K.-K. Kim, S.-J. Park, and T.-Y. Seong, *Appl. Phys. Lett.*, **83**, 479 (2003).
8. S.-P. Jung, D. Ullery, C.-H. Lin, H. P. Lee, J.-H. Lim, D.-K. Hwang, J.-Y. Kim, E.-J. Yang, and S.-J. Park, *Appl. Phys. Lett.*, **87**, 181107 (2005).
9. S.-M. Pan, R.-C. Tu, Y.-M. Fan, R.-C. Yeh, and J.-T. Hsu, *IEEE Photon. Technol. Lett.*, **15**, 646 (2003).
10. H. K. Cho, T. Hossain, J. W. Bae, and I. Adesida, *Solid-State Electron.*, **49**, 774 (2005).
11. G.-T. Chen, C.-C. Pan, C.-S. Fang, T.-C. Huang, J.-I. Chyi, M.-N. Chang, S.-B. Huang, and J.-T. Hsu, *Appl. Phys. Lett.*, **85**, 2797 (2004).
12. J. W. Bae, T. Hossain, I. Adesida, K. H. Bogart, D. Koleske, A. A. Allerman, and J. H. Jang, *J. Vac. Sci. Technol. B*, **23**, 1072 (2005).
13. J.-R. Lee, S.-I. Na, J.-H. Jeong, S.-N. Lee, J.-S. Jang, S.-H. Lee, J.-J. Jung, J.-O. Song, T.-Y. Seong, and S.-J. Park, *J. Electrochem. Soc.*, **152**, G92 (2005).
14. V. Rajagopal Reddy, S.-H. Kim, J.-O. Song, and T.-Y. Seong, *Solid-State Electron.*, **48**, 1563 (2004).
15. J.-S. Jang, S.-J. Park, and T.-Y. Seong, *Appl. Phys. Lett.*, **76**, 2898 (2000).
16. J.-S. Jang, D.-J. Kim, S.-J. Park, and T.-Y. Seong, *J. Electron. Mater.*, **30**, 94 (2001).
17. H. W. Jang, W. Urbanek, M. C. Yoo, and J.-L. Lee, *Appl. Phys. Lett.*, **80**, 2937 (2002).
18. H. W. Jang and J.-L. Lee, *J. Appl. Phys.*, **93**, 5416 (2003).
19. J. O. Song, D.-S. Leem, J. S. Kwak, O. H. Nam, Y. Park, and T.-Y. Seong, *Appl. Phys. Lett.*, **83**, 2372 (2003).
20. J. Narayan, H. Wang, T.-H. Oh, H. K. Choi, and J. C. C. Fan, *Appl. Phys. Lett.*, **81**, 3978 (2002).
21. H. W. Jang, S. Y. Kim, and J.-L. Lee, *J. Appl. Phys.*, **94**, 1748 (2003).
22. M.-S. Oh, D.-K. Hwang, J.-H. Lim, C.-G. Kang, and S.-J. Park, *Appl. Phys. Lett.*, **89**, 042107 (2006).
23. W. S. Wong, T. Sands, N. W. Cheung, M. Kneissl, D. P. Bour, P. Mei, L. T. Romano, and N. M. Johnson, *Appl. Phys. Lett.*, **77**, 2822 (2000).
24. T. Fujii, Y. Gao, R. Sharma, E. L. Hu, S. P. DenBaars, and S. Nakamura, *Appl. Phys. Lett.*, **84**, 855 (2004).
25. *CRC Handbook of Chemistry and Physics*, 83rd ed., D. R. Lide, Editor, CRC, New York (2002).
26. J.-O. Song, J. S. Kwak, Y. Park, and T.-Y. Seong, *Appl. Phys. Lett.*, **86**, 062104 (2005).
27. H. W. Jang, J. H. Son, and J.-L. Lee, *Appl. Phys. Lett.*, **90**, 012106 (2007).
28. S. Lee, J. H. Son, G. H. Jung, Y. G. Kim, C. Y. Kim, Y. J. Yoon, and J.-L. Lee,

Appl. Phys. Lett., **91**, 222115 (2007).
29. S. Kim, J.-H. Jang, and J.-S. Lee, *J. Electrochem. Soc.*, **154**, H973 (2007).
30. D.-S. Leem, T.-W. Kim, T. Lee, J.-S. Jang, Y.-W. Ok, and T.-Y. Seong, *Appl. Phys. Lett.*, **89**, 262115 (2006).
31. J.-O. Song, J. S. Kwak, and T.-Y. Seong, *Appl. Phys. Lett.*, **86**, 062103 (2005).
32. C. H. Chou, C. L. Lin, Y. C. Chuang, H. Y. Bor, and C. Y. Liu, *Appl. Phys. Lett.*, **90**, 022103 (2007).
33. J.-Y. Kim, S.-I. Na, G.-Y. Ha, M.-K. Kwon, I.-K. Park, M.-H. Kim, D. Choi, and K. Min, *Appl. Phys. Lett.*, **88**, 043507 (2006).
34. J. F. Moulder, W. F. Strickle, P. E. Sobol, and K. D. Bomben, *Handbook of X-Ray Photoelectron Spectroscopy*, Perkin-Elmer, Eden Prairie, MN (1992).
35. P. J. Hartlieb, A. Roskowski, R. F. Davis, W. Platow, and R. J. Nemanich, *J. Appl. Phys.*, **91**, 732 (2002).
36. H. K. Kim, H. W. Jang, and J.-L. Lee, *J. Appl. Phys.*, **98**, 104309 (2005).
37. G. F. Malgas, D. Adams, P. Nguyen, Y. Wang, T. L. Alford, and J. W. Mayer, *J. Appl. Phys.*, **90**, 5591 (2001).
38. D. A. Porter and K. E. Easterling, *Phase Transformations in Metals and Alloys*, Chapman & Hall, London (1992).
39. F. R. de Boer, R. Boom, W. C. M. Mattens, A. R. Miedema, and A. K. Niessen, *Cohesion in Metals*, North-Holland, Amsterdam (1988).